

# **ICPES 2025**

# 40<sup>th</sup> INTERNATIONAL CONFERENCE ON PRODUCTION ENGINEERING - SERBIA 2025

DOI: 10.46793/ICPES25.384B



University of Nis
Faculty of Mechanical
Engineering

Nis, Serbia, 18 - 19th September 2025

# ADVANCED DESIGN OF 3D-PRINTED COMPONENTS FOR ROBOTIC END-EFFECTORS: A TAGUCHI-BASED MASS AND VOLUME OPTIMIZATION

Dejan BOZIC<sup>1</sup>, Mijodrag MILOSEVIC<sup>1</sup>, Zeljko SANTOSI<sup>1</sup>, Grigor STAMBOLOV<sup>2</sup>, Dejan LUKIC<sup>1\*</sup>

 $\textbf{Orcid:}\ 0009\text{-}0009\text{-}1095\text{-}8101;\ \textbf{Orcid:}\ 0000\text{-}0002\text{-}8950\text{-}4867;\ \textbf{Orcid:}\ 0000\text{-}0003\text{-}3975\text{-}0864;\\$ 

Orcid: 0000-0002-1566-282X

<sup>1</sup>University of Novi Sad, Faculty of Technical Sciences, Department of Production Engineering, Novi Sad, Serbia

> <sup>2</sup>Technical University of Sofia, Faculty of Industrial Technology, Sofia, Bulgaria \*Corresponding author: lukicd@uns.ac.rs

Abstract: This study investigates the optimization of mass and volume in 3D-printed components featuring internal lattice structures, using the Taguchi method and Fused Deposition Modeling (FDM) technology. A set of three design parameters-unit cell type, cell size, and shell thickness-was systematically varied across three levels using an L9 orthogonal array. The goal was to identify combinations that minimize material usage without compromising structural integrity. Lattice structures were designed and generated using nTop software, which enabled efficient modeling of complex geometries through implicit modeling and field-driven design techniques. Experimental results showed that cell size had the most significant effect on both mass and volume reduction, while the Diamond unit cell type and reduced shell thickness further contributed to performance improvement. Statistical analysis, including signal-to-noise (S/N) ratio evaluation and ANOVA, confirmed the robustness of the identified optimal configuration. The results underscore the potential of combining advanced design tools with structured experimental methods to accelerate material-efficient product development in additive manufacturing.

Keywords: robotic arm, 3D scan, Optimization, 3D Printing, Physical adaptation.

### 1. INTRODUCTION

This paper presents a multidisciplinary approach to adapting an existing industrial robot for 3D scanning applications, involving the development of a custom-designed interface (gripper) to connect the robot with the scanner. The gripper was specifically engineered for this purpose and fabricated using additive manufacturing (3D printing).

The primary aim of the project was to extend the functionality of existing industrial equipment through the integration of modern digital tools and advanced manufacturing technologies.

The second section provides a comprehensive literature review related to industrial robots, additive manufacturing technologies, and CAD model search engines. The third section, titled *Materials and Methods*, outlines the design workflow for the

gripper, introduces the selected robot and scanner, and describes the reverse engineering process. It also details the use of the 3DfindIT platform for identifying similar components, along with the final modified and adapted gripper design.

The fourth section presents the experimental setup and results, including a Taguchi design of experiments followed by ANOVA analysis for systematic parameter evaluation. Finally, the fifth section summarizes the key findings and implications of the study.

#### 2. LITERATURE REVIEW

Industrial robots, defined by ISO 8373:2021 as reprogrammable, multipurpose manipulators controlled along three or more axes and capable of being either fixed or mobile [1], remain a key element in large-scale manufacturing processes [2]. They are widely categorized into six types: Polar, Cylindrical, Cartesian, SCARA, Vertically Articulated, and Parallel-Link robots [3,4]. Their economic efficiency has been demonstrated across various industrial fields, with validation from multiple studies and practical applications [2,5-7].In the shift toward smart manufacturing, industrial robots are increasingly embedded within digital ecosystems such as Industry 4.0 [8], the Internet of Things (IoT), Cyber-Physical Systems, and Big Data frameworks [9,10]. This integration supports automation, predictive analytics, and real-time process control [11,12]. A critical part of this digital evolution involves 3D digital models, which are central to digital twins used for simulating real-world industrial scenarios [13,14,15]. progression toward sustainability in robotics depends heavily on modernizing outdated robotic systems. One effective strategy involves replacing obsolete control units with newer ones that enhance motion planning and allow for complex operations [1]. Through IoT connectivity, robots can be monitored and remotely operated via applications [16]. Old robotic arms, which

often remain unused, can be revitalized for simple industrial tasks such as sorting, welding, and assembly [17,18]. In educational settings, they also serve as practical tools for student training in programming, sensor systems, and automation logic [19]. Flexible deployment is becoming increasingly essential in manufacturing environments characterized mass customization. Reconfigurable manufacturing systems (RMSs) promote adaptability, where robots and machines are repositioned as needed [20]. This evolution encourages the reuse of existing systems and contributes to circular technological practices. A major contributor to robotic adaptability is the design and functionality of end-effectors, particularly grippers. Traditional hard grippers are well suited to structured geometries but are limited when handling irregular shapes [21]. In contrast, soft robotic grippers, actuated by pneumatic systems, cable-driven mechanisms, or shape memory alloys, offer greater versatility and a gentler touch-ideal for fragile or non-uniform objects [9,22]. Robotic arms equipped with 3D scanning systems are instrumental in modern quality control processes, especially in metrology [23]. These systems help improve product accuracy, reduce manufacturing time, and lower operational costs [24-27]. A specialized method proposed by Ma et al. [28] combines a linear laser scanner and a laser cladding nozzle mounted on a robot to restore worn free-form surfaces. Another vision-based solution utilizes multiple cameras reconstruct 3D point clouds and align them with CAD models, significantly increasing positioning accuracy in dynamic environments [29]. The versatility of industrial robots also enables their use in cutting-edge research. For instance, they have been used to study the effects of cutting parameters on fibber quality during ultrasonic cutting [30]. Additionally, the integration of robotic systems with additive techniques manufacturing like Fused Deposition Modelling (FDM) offers new opportunities for free-form fabrication [31]. This study addresses a unique and practical challenge-how to adapt older articulated

robotic arms to function with handheld 3D scanners. Unlike modern systems, these legacy robots lack direct compatibility with handheld devices, which are typically not intended for robotic integration. However, through a multidisciplinary approach that includes photogrammetry-based 3D digitization, reverse engineering (RE), CAD modelling using SolidWorks, the use of CAD component search engines (3Dfindit), and FDM 3D printing, aviable integration can be achieved.

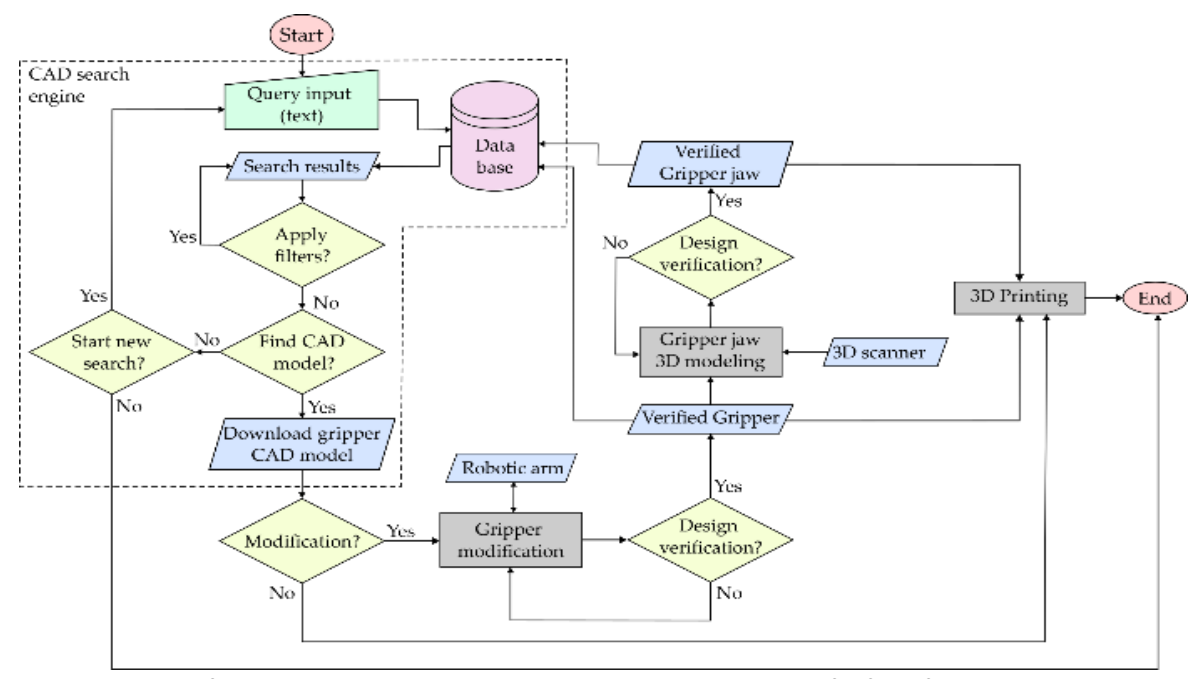
#### 3. MATERIALS AND METHODS

Figure 1. illustrates the workflow for designing a fully functional 3D-printed connector for robotic grippers. The process begins by querying online CAD platforms such as 3Dfindit (CADENAS GmbH, Augsburg, Germany) [32], which enables access to a wide range of verified 3D models from numerous manufacturer catalogues [33-35]. Searches can be refined using filters like file format, dimensions, category, or manufacturer, and can include inputs such as keywords, images, sketches, or existing CAD files [36].

If a suitable CAD model is located, it is downloaded and assessed for compatibility. In cases where adjustment is needed to suit 3D printing or ensure structural integrity, the model is modified-typically to improve strength-to-weight ratio or to match the unique geometry of a specific 3D scanner [37,38].

Once modified, a design verification stage the gripper satisfies requirements for integration with the robotic arm and the 3D scanner. If not, further refinements are made. Due to the variability in scanner shapes and materials (most commercial grippers are metal, unlike typical 3D-printed plastic ones), custom modelling is often required. This combines the scanner's CAD model with the verified gripper to design jaws that ensure a secure and ergonomic grip.

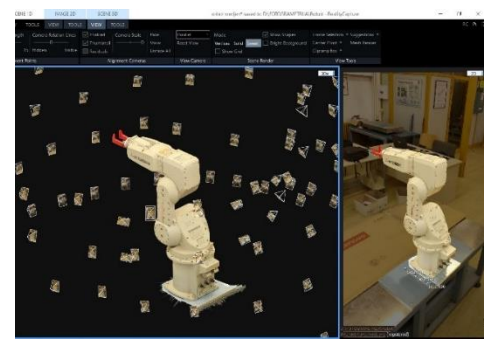
After successful validation, the finalized design is prepared for 3D printing and stored in a shared database for future use or distribution. If any issue is detected during verification, the design returns to the modelling phase for correction.



**Figure 1.** Workflow diagram illustrating the development process of a fully functional 3D-printed connection element [39]

To establish a precise mechanical connection between the Mitsubishi RV-3SDB-S15 robotic

arm (Figure 2a) and the EinScan Pro 2X handheld 3D scanner (Figure 2b), photogrammetric 3D reconstruction methodology was employed. High-resolution images were captured using a Canon EOS 1200D camera, consistently mounted on a tripod to ensure stability and uniform image acquisition. The robotic arm was documented from five concentric levels to achieve full geometric coverage, while the scanner was photographed using a controlled rotary table setup. In total, 169 images were taken for the robot and 37 for the scanner. Coded markers with known, predefined distances were strategically positioned around both objects to provide spatial scale, enabling accurate 3D reconstruction. These markers were automatically detected by photogrammetry software. The resulting high-fidelity 3D models served as essential geometric references for designing a custom-fit connector, physically linking the robot and scanner. This approach enabled precise mechanical adaptation, overcoming the lack of standardized interface compatibility between the two components.



a) Mitsubishi RV-3SDB-S15



b) Shining 3D EinScan Pro 2X optical 3D scanner.
 Figure 2. Physical components used for 3D digitization

Reverse engineering was performed utilizing a combination of CAD modeling techniques, based on 3D mesh references of both the robotic arm and the scanner. SolidWorks 2022 was employed to reconstruct geometric features by extracting precise distances and angles directly from the imported mesh data. Dimensionally accurate CAD models were subsequently generated, with particular attention given to the robotic arm's endeffector interface to ensure proper connector assembly and integration (Figure 3).



a) Robotic arm



b) Optical 3D scanner

Figure 3. Polygonal mesh models

To access the 3Dfindit platform, users are required to be registered and logged in. Figure 4 illustrates the interface showing the final search results. Initially, the term "gripper" was entered into the search bar (Frame 1), returning approximately 25,000 results. To narrow the selection, filters were applied using the keywords "flexible" and "robot" with the "AND" operator (Frame 2), which reduced the matches

to three. The first result was then selected for detailed review (Frame 3).

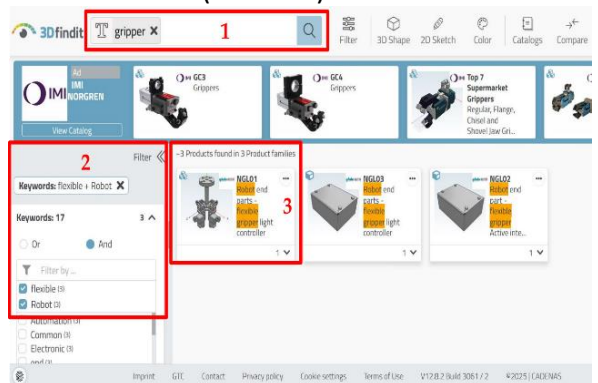


**Figure 4.** Gripper search results on 3Dfindit after applying filter criteria [39]

The selected gripper model was thoroughly examined; its dimensions and cross-sections were verified, and all available documentation was reviewed. After confirmation, the CAD file was downloaded for subsequent modification. Adjustments included resizing the gripper body to accommodate the fixing screws and removing the original flexible jaws. A new jaw block was then modeled to fit the 3D scanner handle with precision, followed by a Boolean intersection operation. The finalized jaw and complete gripper assembly (Figure incorporated all essential geometric features.

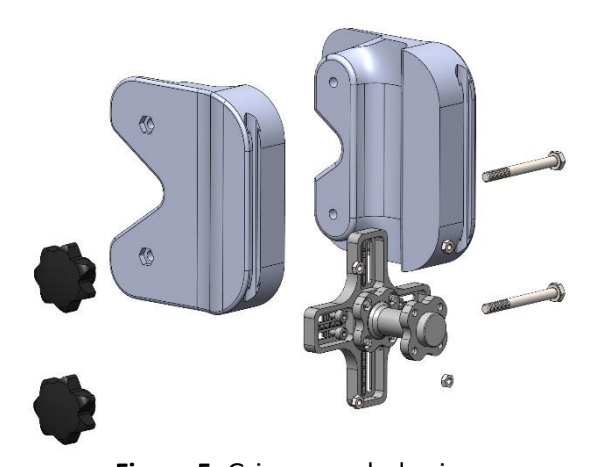


Figure 5. Gripper explode view

## 4. EXPERIMENTAL RESEARCH

In this study, three key design parameters were selected as control factors for the Taguchi experimental design: unit cell type, cell size, and shell thickness. Each factor was assigned three levels based on practical relevance and variation in structural behavior. The unit cell

types (Octet, Diamond, and Hexagonal Honeycomb) represent distinct lattice geometries. Cell sizes of 2 mm, 4 mm, and 6 mm were chosen to evaluate the influence of scale, while shell thicknesses of 1 mm, 2 mm, and 3 mm reflect typical manufacturing boundaries in FDM printing. These combinations form the basis of the L9 orthogonal array used in the experiment (Table 1.).

Table 1. Factors and factor level

Factors	Level 1	Level 2	Level 3
Unit cell (mm)	Octet	Diamond	Hexagonal honeycomb
Cell size (mm)	2	4	6
Shell thickness (mm)	1	2	3

Software nTop was selected for this study due to its advanced capabilities in modeling complex geometries and supporting efficient design workflows, particularly in the context of additive manufacturing. In contrast traditional CAD platforms, which are often limited when working with intricate lattice structures and organic forms, nTop employs an implicit modeling engine. This enables the generation and manipulation of highly complex structures with enhanced computational efficiency and robustness, regardless geometry size or resolution. Its field-driven design methodology allows for the integration of performance data-such as stress, temperature, or displacement fields-directly into geometry creation, resulting in functionally optimized and adaptable parts. This is especially important for lattice structures, where performance is highly dependent on localized behavior. Furthermore, nTop supports parametric control and conditional logic, enabling users to build reusable, logicbased workflows that adapt to new design inputs. Additionally, its robust automation facilitate rapid features iteration and exploration of design variants, significantly reducing the time from concept to optimized part. This makes it particularly suitable for research environments where multiple design configurations need to be evaluated quickly and systematically. The platform's scalability and stability also make it a valuable tool for developing lightweight, performance-driven components across industries such as aerospace, biomedical, and automotive (Figure 6).

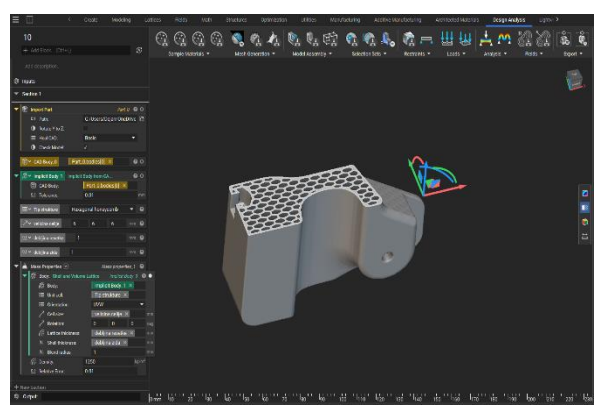


Figure 6. nTop interface

е

### 5. RESULTS AND DISCUSSION

Figure 7. shows the influence of each factor on the signal-to-noise (S/N) ratio for the response "mass". According to the "smaller is better" Taguchi criterion, higher S/N values indicate lower and more stable mass. The analysis reveals that cell size (CELL SIZE) has the most significant influence on the S/N ratio, followed by unit cell type, while shell thickness shows the least influence. The trend indicates that a larger cell size (6 mm) and a diamond-type unit cell contribute to a lower and more consistent mass. Shell thickness has a minor effect in this case.

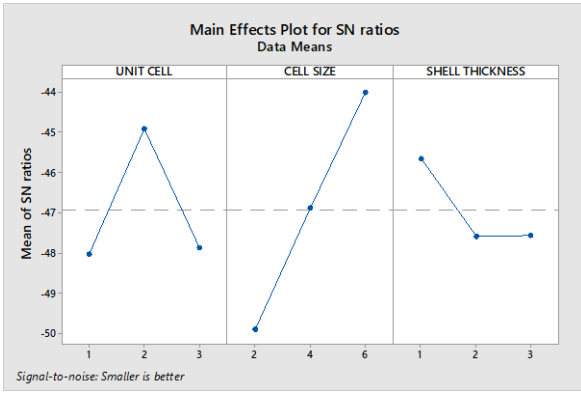


Figure 7. Main Effects Plot for SN ratios

Figure 8. presents the mean mass values for each level of the three input factors. It visually confirms the trends observed in the S/N ratio diagram. The lowest mean mass is achieved when the cell size is large (6 mm), the shell thickness is minimal (1 mm), and the unit cell type is Diamond (level 2). The cell size has the greatest effect on the reduction of part mass, with a clear decreasing trend from 2 mm to 6 mm.

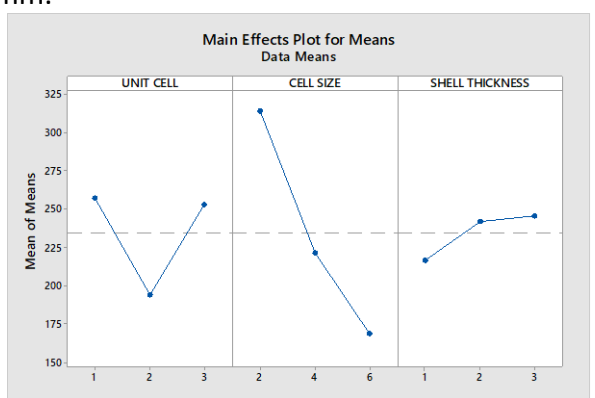
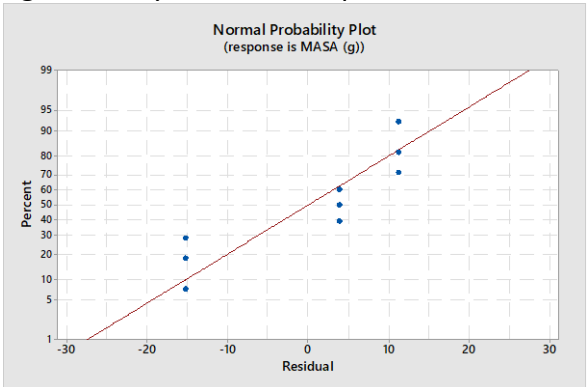


Figure 8. Main Effects Plot for Means

Although the same Taguchi analysis was performed for the response "volume", the Main Effects Plots for S/N ratios and means for volume were found to be visually identical in shape to those for mass. This is expected, since mass and volume are directly proportional for a given material (PLA) with constant density. Therefore, only the plots for mass are shown, as they are fully representative of the trends in both responses.

Figure 9. assesses the normality of residuals in the regression model. The points approximately follow a straight line, indicating that the residuals are normally distributed. This validates the use of the general linear model and confirms the statistical adequacy of the Taguchi analysis for the response mass.



## Figure 9. Normal Probability Plot

This diagram shows the residuals plotted against the fitted values from the model. The distribution of points is random, without any clear pattern, which indicates homoscedasticity (constant variance) and the absence of systematic error. This further confirms that the assumptions of the linear model are satisfied.

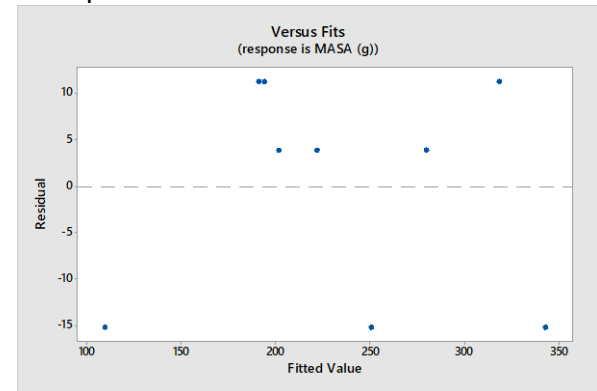


Figure 10. Versus Fits

Residual plots for the "volume" response are not shown because no general linear model was constructed for this response in Minitab. The ANOVA and regression analysis were only performed for the mass variable. As such, residual analysis is only valid and meaningful for mass.

Figure 11 provides a visual representation of the key stages in the additive manufacturing process, specifically utilizing Fused Deposition Modeling (FDM) technology. The image shows a 3D printer in operation, where thermoplastic filament is accurately extruded and deposited layer by layer following a digital model. This layer-by-layer approach enables the fabrication of geometrically complex parts, including intricate internal lattice structures that are often unachievable through traditional manufacturing techniques. The precise control of the extruder's movement ensures accurate material placement, which is essential for achieving the desired dimensional accuracy and mechanical performance of the printed component.

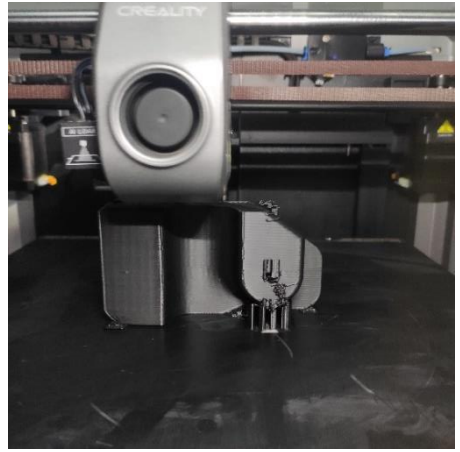


Figure 11. 3D printing process

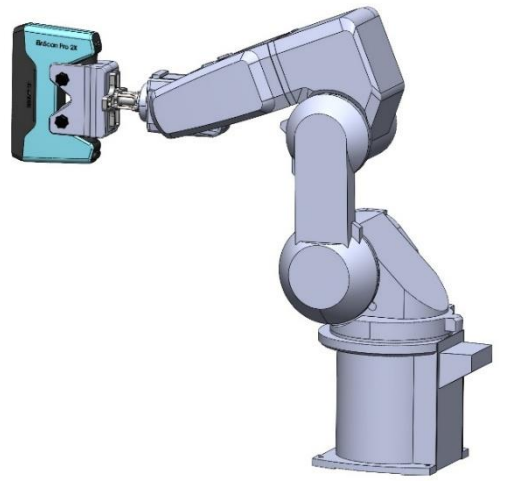
Figure 12 displays the final output of the 3D process-prototype components incorporating optimized lattice structures. These parts reflect the effective application of the Taguchi method, specifically through an L9 orthogonal array, to minimize both mass and volume. The image distinctly illustrates different unit cell types (e.g., Diamond, Octet, and Hexagonal Honeycomb) and emphasizes variations in parameters such as cell size and shell thickness. This visual evidence highlights the capability of FDM technology to fabricate complex internal geometries that enhance material efficiency and contribute to improved overall part performance.



Figure 12. 3D Printing results

The final stage involved assembling the 3D scanner and the modified gripper onto the endeffector of the robotic arm. This integration ensured that all components were properly aligned and mechanically compatible. Figure 13a presents the fully assembled CAD model, serving as a digital twin for virtual validation

and simulation, while Figure 13b depicts the realized physical assembly, confirming the feasibility of the designed connection in real-world conditions.



a) Digital Twin



b) Real system

Figure 13. Adopted articulated robotic arm [39]

## 6. CONCLUSION

This study successfully demonstrated the application of the Taguchi method for optimizing the mass and volume of 3D-printed lattice structures using FDM technology. Among the evaluated parameters, cell size showed the most significant influence on performance. The use of advanced design tools such as nTop proved effective for generating complex, material-efficient geometries. Future research will focus on exploring additional unit cell configurations, incorporating mechanical testing, and integrating new software tools and simulation environments to further enhance optimization workflows and validate functional

performance across a broader range of applications.

#### **FUNDING**

This research has been supported by the Ministry of Science, Technological Development and Innovation (Contract No. 451-03-137/2025-03/200156) and the Faculty of Technical Sciences, University of Novi Sad through project "Scientific and Artistic Research Work of Researchers in Teaching and Associate Positions at the Faculty of Technical Sciences, University of Novi Sad 2025" (No. 01-50/295. Also, this paper is part of a study in the project "Collaborative systems in the digital environment" industrial No. 142-451-3178/2022-01/01, supported by the Provincial Secretariat for Higher Education and Scientific Research of the Autonomous Province of Vojvodina.)

### **ACKNOWLEDGEMENT**

This research has been supported by the Department of Production Engineering, Faculty of Technical Sciences, University of Novi Sad through project "The future of production engineering".

#### REFERENCES

- [1] ISO 8373:2021; Robotics—Vocabulary. International Organization for Standardization: Geneva, Switzerland, 2021.
- [2] Yin, X.; He, W.; Wang, J.; Peng, S.; Cao, Y.; Zhang, B. Health State Assessment Based on the Parallel–Serial Belief Rule Base for Industrial Robot Systems. Eng. Appl. Artif. Intell. 2025, 142, 109856.
  - https://doi.org/10.1016/j.engappai.2024.10985 6.
- [3] Singh, G.; Banga, V.K. Robots and Its Types for Industrial Applications. Mater. Today Proc. 2022, 60, 1779–1786. https://doi.org/10.1016/j.matpr.2021.12.426.
- [4] The Basics of Industrial Robots Industrial Robots by Kawasaki Robotics. Available online: https://kawasakirobotics.com/asia-oceania/industrial-robots/ (accessed on 4 January 2025).

- [5] Onstein, I.F.; Bjerkeng, M.; Martinsen, K. Automated Tool Trajectory Generation for Robotized Deburring of Cast Parts Based on 3D Scans. Procedia CIRP 2023, 118, 507–512. https://doi.org/10.1016/j.procir.2023.06.087.
- [6] Khoat, N.X.; Hoa, C.T.V.; Khoa, N.B.N.; Dung, N.M. Trajectory Planning and Tracking Control for 6-DOF Yaskawa Manipulator Based on Differential Inverse Kinematics. J. Robot. Control (JRC) 2024, 5, 2035–2047. https://doi.org/10.18196/jrc.v5i6.23109.
- [7] Ulrich, M.; Steger, C.; Butsch, F.; Liebe, M. Vision-Guided Robot Calibration Using Photogrammetric Methods. ISPRS J. Photogramm. Remote Sens. 2024, 218, 645–662.

https://doi.org/10.1016/j.isprsjprs.2024.09.037

.

- [8] Milošević, M.; Lukić, D.; Borojević, S.; Antić, A.; Đurđev, M. A Cloud-Based Process Planning System in Industry 4.0 Framework. In Proceedings of the 4th International Conference on the Industry 4.0 Model for Advanced Manufacturing; Lecture Notes in Mechanical Engineering; Springer: Cham, Switzerland, pp. 202–211, 2019. https://doi.org/10.1007/978-3-030-18180-2\_16.
- [9] Xu, Y.; Lv, M.; Xu, Q.; Xu, R. Design and Analysis of a Robotic Gripper Mechanism for Fruit Picking. Actuators 2024, 13, 338. https://doi.org/10.3390/act13090338.
- [10] Oks, S.J.; Jalowski, M.; Lechner, M.; Mirschberger, S.; Merklein, M.; Vogel-Heuser, B.; Möslein, K.M. Cyber-Physical Systems in the Context of Industry 4.0: A Review, Categorization and Outlook. Inf. Syst. Front. 2024, 26, 1731–1772. https://doi.org/10.1007/s10796-022-10252-x.
- [11] Stepanić, P.; Dučić, N.; Stanković, N. Development of Artificial Neural Network Models for Vibration Classification in Machining Process on Brownfield CNC Machining Center. J. Prod. Eng. 2024, 27, 16–20. https://doi.org/10.24867/JPE-2024-02-016.
- [12] Hozdić, E.; Makovec, I. Evolution of the Human Role in Manufacturing Systems: On the Route from Digitalization and Cybernation to Cognitization. Appl. Syst. Innov. 2023, 6, 49. https://doi.org/10.3390/asi6020049.
- [13] Kamali, M.; Atazadeh, B.; Rajabifard, A.; Chen, Y. Advancements in 3D Digital Model Generation for Digital Twins in Industrial Environments: Knowledge Gaps and Future

- Directions. Adv. Eng. Inform. 2024, 62, 102929. https://doi.org/10.1016/j.aei.2024.102929.
- [14] Chen, K.; Zhao, B.; Zhang, Y.; Zhou, L.; Niu, K.; Jin, X.; Xu, B.; Yuan, Y.; Zheng, Y. Digital Twin-Based Vibration Monitoring of Plant Factory Transplanting Machine. Appl. Sci. 2023, 13, 12162.
  - https://doi.org/10.3390/app132212162.
- [15] Wang, Z.; Wang, L.; Martínez-Arellano, G.; Griffin, J.; Sanderson, D.; Ratchev, S. Digital Twin Based Photogrammetry Field-of-View Evaluation and 3D Layout Optimisation for Reconfigurable Manufacturing Systems. J. Manuf. Syst. 2024, 77, 1045–1061. https://doi.org/10.1016/j.jmsy.2024.11.001.
- [16] Laman, E.; Maslan, M.N.; Ali, M.M.; Abdullah, L.; Zamri, R.; Syafiq, M.; Mohamed, S.; Zainon, M.; Noorazizi, M.S.; Sudianto, A. Design of an Internet of Things Based Electromagnetic Robotic Arm for Pick and Place Applications. Malays. J. Compos. Sci. Manuf. 2020, 2, 12–20.
- [17] Fitria, S.; Nawawi, Z.; Kurnia, R.F.; Yuniarti, D.; Dewi, T. Simulation of Robot Arm System Control Using Fuzzy Logic. Sriwij. Electr. Comput. Eng. J. 2024, 1, 20–29. https://doi.org/10.62420/selco.v1i1.2.
- [18] Elfasakhany, A.; Yanez, E.; Baylon, K.; Salgado, R. Design and Development of a Competitive Low-Cost Robot Arm with Four Degrees of Freedom. Mod. Mech. Eng. 2011, 01, 47–55. https://doi.org/10.4236/mme.2011.12007.
- [19] Yusoff, Z.M.; Nordin, S.A.; Markom, A.M.; Mohammad, N.N. Wireless Hand Motion Controlled Robotic Arm Using Flex Sensors. Indones. J. Electr. Eng. Comput. Sci. 2023, 29, 133–140.
  - https://doi.org/10.11591/ijeecs.v29.i1.
- [20] Arnarson, H. Intelligent Self- and Reconfigurable Manufacturing System. Ph.D. Thesis, UiT The Arctic University of Norway, Tromsø, Norway, 2023.
- [21] Diller, E.; Sitti, M. Three-Dimensional Programmable Assembly by Untethered Magnetic Robotic Micro-Grippers. Adv. Funct. Mater. 2014, 24, 4397–4404. https://doi.org/10.1002/adfm.201400275.
- [22] Milojević, A.; Linß, S.; Ćojbašić, Ž.; Handroos, H. A Novel Simple, Adaptive, and Versatile Soft-Robotic Compliant Two-Finger Gripper With an Inherently Gentle Touch. J. Mech. Robot. 2021, 13, 011015. https://doi.org/10.1115/1.4048752.

- [23] Dzedzickis, A.; Subačiūtė-Žemaitienė, J.; Šutinys, E.; Samukaitė-Bubnienė, U.; Bučinskas, V. Advanced Applications of Industrial Robotics: New Trends and Possibilities. Appl. Sci. 2021, 12, 135. https://doi.org/10.3390/app12010135.
- [24] Vasiljević, S.; Rajković, D.; Đorđević, M.; Kostić, S.; Stanojević, M. Application of Innovative Mechatronic Systems in Product Design, Development and Production. J. Prod. Eng. 2024, 27, 13–21. https://doi.org/10.24867/jpe-2024-01-013.
- [25] Zong, Y.; Liang, J.; Pai, W.; Ye, M.; Ren, M.; Zhao, J.; Tang, Z.; Zhang, J. A High-Efficiency and High-Precision Automatic 3D Scanning System for Industrial Parts Based on a Scanning Path Planning Algorithm. Opt. Lasers Eng. 2022, 158, 107176. https://doi.org/10.1016/j.optlaseng.2022.1071 76
- [26] Zheng, Y.; Liu, W.; Zhang, Y.; Ding, H.; Li, J.; Lu, Y. Laser In-Situ Measurement in Robotic Machining of Large-Area Complex Parts. Measurement 2025, 241, 115718. https://doi.org/10.1016/j.measurement.2024.1 15718.
- [27] Itadera, S.; Domae, Y. Motion Priority Optimization Framework towards Automated and Teleoperated Robot Cooperation in Industrial Recovery Scenarios. Robot. Auton. Syst. 2025, 184, 104833. https://doi.org/10.1016/j.robot.2024.104833.
- [28] Ma, W.; Hu, T.; Zhang, C.; Chen, Q. Adaptive Remanufacturing for Freeform Surface Parts Based on Linear Laser Scanner and Robotic Laser Cladding. Robot. Comput.-Integr. Manuf. 2025, 91, 102855. https://doi.org/10.1016/j.rcim.2024.102855.
- [29] Wu, J.; Jiang, H.; Wang, H.; Wu, Q.; Qin, X.; Vision-Based Dong, Multi-View K. Reconstruction for **High-Precision** Part Positioning in Industrial Robot Machining. Measurement 2025, 242, 116042. https://doi.org/10.1016/j.measurement.2024.1 16042.

[30] Gu Kim, H.; Hwa Hong, T.; Kim, D.; Hyeon Kim, S. An Experimental Study of Ultrasonic-Knife Cutting for a Woven Carbon Fiber Preform by an Industrial Robot. Manuf. Lett. 2024, 41, 581– 587.

https://doi.org/10.1016/j.mfglet.2024.09.074.

- [31] Toshev, R.; Bengs, D.; Helo, P.; Zamora, M. Advancing Free-Form Fabrication: Industrial Robots' Role in Additive Manufacturing of Thermoplastics. Procedia Comput. Sci. 2024, 232, 3131–3140. https://doi.org/10.1016/j.procs.2024.02.129.
- [32] CAD Content Platform for Engineers, Architects, Purchasers. Available online: https://www.3dfindit.com/en/ (accessed on 15 December 2024).
- [33] 3D Models and Modelling Software | MacOdrum Library. Available online: https://library.carleton.ca/services/3d-printing/3d-models-and-modelling-software (accessed on 10 January 2025).
- [34] 3D Models Search Engines in 2024—Asseter. Available online: https://asseter.ai/3d-models-search-engines-in-2024/ (accessed on 10 January 2025).
- [35] 7 Best Search Engines for 3d Printing Models. Available online: https://www.3ddrucklife.de/post/7-best-search-engines-for-3d-printing-models-stl-finder?srsltid=AfmBOoqasBLO9oMsiNokwx2T\_uvyL1f2gU2rQsSOU6rttVIAZus7Z2hw (accessed on 10 January 2025).
- [36] Get Started With 3Dfindit. Available online: https://www.3dfindit.com/en/engiclopedia/etstarted-with-3-dfindit (accessed on 10 January 2025).
- [37] Perak, V. Influence of infill density and number of layers on mechanical properties of 3D printed pla and abs sandwich. *Adv. Eng. Lett.* **2024**, *3*, 154–163.
- [38] Hozdić, E. Characterization and Comparative Analysis of Mechanical Parameters of FDM- and SLA-Printed ABS Materials. *Appl. Sci.* **2024**, *14*, 649. <a href="https://doi.org/10.3390/app14020649">https://doi.org/10.3390/app14020649</a>.